

## Analyzing the Failure of Master Mould in Casting of Copper Anode Moulds and Suggesting a more Suitable Metal Mould

M. Adjabshiri and S. Sharafi\*

Materials Science and Engineering Department, Shahid-Bahonar University of Kerman, Iran

Received July 22, 2006; Accepted November 6, 2006

### Abstract

Master moulds are used to cast copper anode moulds. These moulds are made of grey or nodular cast irons, because they possess the desired properties. It was expected that ductile cast iron moulds could have performed their nominal life. But in service, these moulds have not performed their nominal life and they have experienced premature failures due to warping and cracking. Also grey cast iron moulds fail because of generalized surface cracks. In this paper, the failure of master moulds is investigated according to the metallographic and hardness measurement tests. Then pearlitic and austempered ductile iron alloys are proposed and tested through short time high temperature tensile and thermal shock tests similar to working conditions of the moulds. Also master mould is modeled by Finite Element Method to evaluate the thermal conditions. Finally it is concluded that compared with pearlitic ductile iron, austempered ductile iron has higher resistance to thermal shock.

*Keywords:* Master mould, Bainitic ductile cast iron, Thermal shock

### Introduction

In copper melting plants, sulphur concentrates are melted in Reverb furnaces to form copper matt. Copper matt is converted to blister copper in a converter, by passing through thermal refining processes, and then is cast to form anode plates. Then anodes pass electrical refining processes to form pure copper<sup>1)</sup>. Anodes weigh nearly 350kg, they are approximately square in shape with about 4-5 cm thickness and have an area of approximately 1m<sup>2</sup> on each side. The cast anodes have lugs for suspending them in electrical cells (Figure 1). The casting process of anode is done in the copper moulds which is placed on the molding wheels to obtain copper anodes.

Cast iron moulds are used to cast copper moulds and are called master mould (Figure 2). The central part of the master mould is shaped in such a way that is a positive of the copper anodes. The raised central section of the master mould which will form the anode is referred to, in the remainder of this paper, as the "anode". Master moulds are made of nodular cast irons with pearlitic matrix or grey cast irons with ferritic matrix. In casting of copper anodic moulds, four frames are placed in the upper side of the master mould, and then the assembly is preheated to about 200 °C.

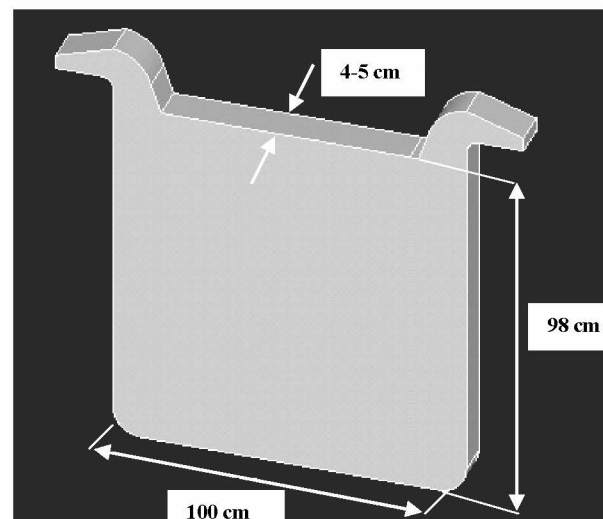


Fig. 1. A view of anodic copper.

Before casting, the surface is covered by a thin layer of barium sulfate and then copper is cast at a temperature in the range of 1180-1220 °C. After solidification of copper mould in about 20 minutes, it is taken out from the master mould and then the master mould is cooled in still air.

The ductile cast iron moulds with pearlitic matrix, warped after 30 casting cycles and sometimes this warping is accompanied by cracking. Grey cast iron moulds with ferritic matrix underwent up to 50 casting cycles, and mainly failed because of generalized surface cracking. In this paper, we have investigated the failure of master mould through metallographic and hardness tests. According to the

\* Corresponding author:

Tel: +98-341-2111-865 Fax: +98-341-2111865

E-mail: Sh\_Sharafi@mail.uk.ac.ir

Address: Dept. of Materials Science and Engineering, Shahid-Bahonar University of Kerman, IRAN

results, two materials have been proposed, one is pearlitic ductile cast iron and the other one is austempered ductile iron. Then we examined these materials by performing short time high temperature tensile and thermal shock tests similar to working conditions of master mould.



Fig. 2. An image of master mould.

## Experimental procedures

### Chemical composition

The chemical composition of the master mould (made of ductile cast iron) is given in Table 1. As it can be seen from this Table, the amount of Mg is less than required (0.06-0.09 wt %) <sup>2)</sup>.

### Metallographic and hardness tests

Two samples were prepared from upper and lower sides of the master mould, one is cut off from the upper side which is in contact with molten copper and the other one from the lower side, which underwent no considerable heat to compare their microstructures. Hardness test was also performed by a portable hardness tester (Equotip2) on various parts of the master mould, including anodic form region and parts away from anodic region. The results will be discussed in section 3. Based on these results two kinds of cast irons, pearlitic and austempered ductile irons were considered to be suitable substitutes. To verify our suggestions, the following experiments were conducted.

### Specimen preparation

24 rod-shaped and 8 mushroom-shaped specimens were prepared industrially by pouring ductile cast iron molten metal into six and two CO<sub>2</sub> sand moulds, respectively. The chemical composition of the ductile iron is given in Table 2. As-cast specimens are shown in Fig. 3a schematically. Then the samples are machined according to ASTM-A370

standard<sup>3)</sup> to final dimensions of tensile and thermal shock specimens, which are shown in Fig. 3b. These specimens were austenitized at 950 °C for thirty minutes in salt bath (NaCl, Na<sub>2</sub>CO<sub>3</sub>, BaCl<sub>2</sub>). Then 12 tensile specimens and 4 thermal shock specimens were normalized in air to obtain pearlitic microstructure. The other specimens including 12 tensile and 4 thermal shock specimens were cooled to austempering temperature in a nitrate bath (sodium nitrate, sodium nitrite, potassium nitrate) at 300 °C rapidly and were kept there for 2 hours to obtain bainitic microstructures.

### Short time high temperature tensile test

High temperature tensile test were conducted at temperatures of 25, 400, 600 and 800 °C. The specimens were prepared according to ASTM-A370 standard and were held at each temperature for five minutes before testing. Tensile tests were performed on an Instron-8502 universal testing machine with a constant strain rate of 2 mm/min. Three tensile tests were made at each test temperature and their results were averaged to evaluate characteristics of the specimens.

### Thermal shock test

There are no standard thermal shock and thermal fatigue tests that have been adopted by industry because each application contains a particular combination of conditions including maximum temperature, temperature difference, stress concentrations, degree of fatigue damage (thermal cracking) tolerable, expected service life, etc<sup>4)</sup>. However test conditions were chosen to simulate actual heating and cooling. Two sets of mushroom-shaped samples with two holes on the top that lead to stress concentration in the bridge between the two holes and initiating crack were prepared, Figure 3. Each set has one pearlitic and one bainitic sample. Also we need a condition to shock specimens severely and at the same time the material of hot environment to prevent from sticking to the samples. Some researchers have used molten salt bath or flame, but molten salt bath has less shock relative to molten copper, and sticks to the samples. Although, the flame induces higher shock than molten copper, it can not be completely controlled and needs special instruments. So, we used molten lead, since this material has a great effect on samples and doesn't stick to them. Holding times of samples in different conditions are given in Table 3 for comparability<sup>5)</sup>. The molten lead was prepared in the electrical resistance furnace and the temperature reached up to 1000 °C similar to conditions of copper pouring into the mould. Also, the molten surface was covered with graphite to prevent oxidation. The surface of samples was inserted in lead for 30 second, then one

set of samples was cooled in the air and the other was quenched in the water. In the process, the surface temperature reached up to 700-800 °C that is similar to working conditions. This process was continued

until crack initiation started in the samples. The number of cycles that cause crack of 1mm length in the bridge between the two holes has been recorded. The results are given in section 3-4.

Table 1. Chemical composition of master mould made of ductile cast iron.

Element	CE	C	Si	Mn	Cu	Mo	Cr	Ni	Mg
wt %	3.81	3.2	1.80	0.34	0.35	0.03	0.16	0.18	0.02

Table 2. Chemical composition of ductile cast iron for as-cast samples.

Element	C	Si	Ni	Mo	Cr	Cu	Fe
Composition (wt%)	3.4	2.4	0.6	0.28	0.1	0.6	balance

Table 3. Holding times of samples in different furnaces [3].

Holding time (in seconds) of samples for one millimeter of diameter and thickness			Furnace temp(°C)	Furnace
Rectangular section	Square section	Rod section		
60-75	50-60	40-50	800	Electrical furnace Salt bath Lead bath Salt bath
18-22	15-18	12-15	800	
10-12	8-10	6-8	800	
10-12	8-10	6-8	1300	

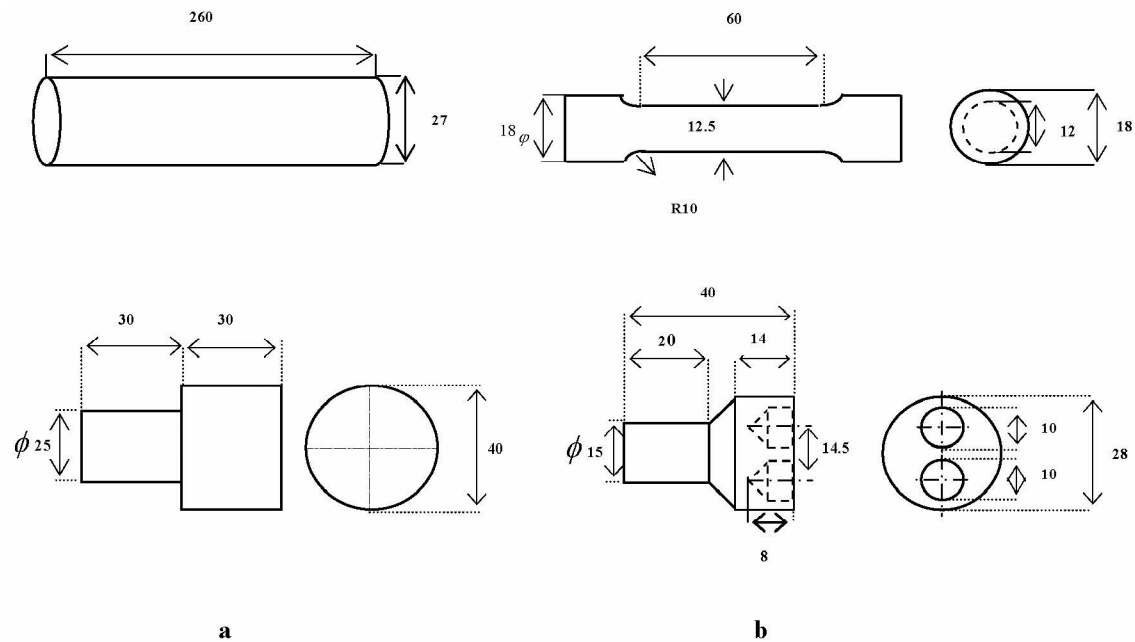


Fig. 3. a) Shape and dimensions of as-cast samples  
b) Shape and dimensions of tensile and thermal shock samples (mm).

**Results and discussion**

*Metallographic and hardness test results*

The results of metallographic tests indicate fairly the nodularity of graphite in the coarse pearlitic matrix of the cross section of the lower part of the master mould as shown in Figure 4 whereas the microstructure of anodic part which is in contact with molten copper is bull's eye graphite in the fine pearlitic matrix (Figure 5). Austenitizing process followed by cooling down in air to normalized state which takes place in every cycle will lead to bull's eye graphite. Also, that of this part is smaller than the graphite of the other parts of master mould that may arise from surface decarburization<sup>6,1)</sup>. In general, the graphite can initiate cracks and propagate them. Results of hardness test are also shown in Figure 6. As we expected, that of anodic part is higher than hardness of the other parts of the mould, that is in good agreement with microstructural differences existing between these parts. The cracks propagation in cast irons can be explained by fracture theory.

*Mechanism of failure*

Heating and cooling of mould causes microstructural changes and phase transformation in

the iron. Cracking is caused by alternating expansion and contraction stresses resulting from this transformation. These cracks are known as crazing, which is the result of thermal fatigue induced by these cyclic thermal stresses. The graphitization of iron carbides and the oxidation of iron also contribute to these stresses<sup>6,1)</sup>. In addition to the above mechanisms, stresses also arise from the expansion and contraction of the mould, simply due to non-homogeneous heating and cooling. The resulting stresses are linked to the expansion coefficient of the material and its elasticity, in particular to the modules of elasticity and Poisson's coefficient. Also, the failure of ductile iron master mould is apparent as a warping of the "anode" area, whose surface becomes concave. An explanation is that warping was caused by the relaxation of elastic stresses. The stresses could be caused by non-homogeneous heating and cooling, for instance, during the casting of the master mould in the sand mould. During the solidification of master mould, uneven contractions in different areas of the cast iron may have caused residual tangential tensile stresses on the top surface of the "anode" which relax when the master mould is in use, giving rise to the concave surface mentioned. Finally, superficial or total breakage of the material will occur depending on its fracture strength<sup>6,1)</sup>.

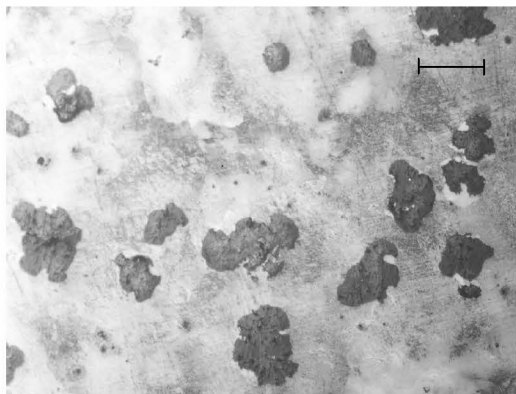


Fig. 4. Microstructure of graphite with different shapes in the coarse pearlitic matrix, (Nital 2%).

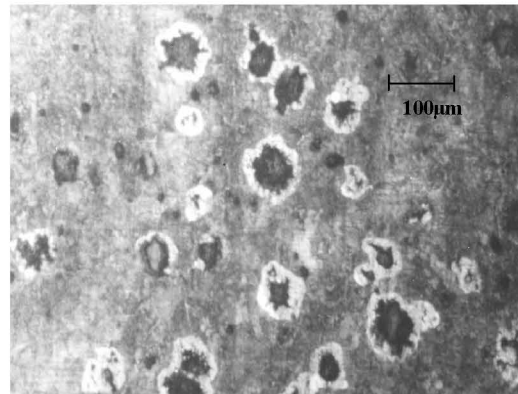
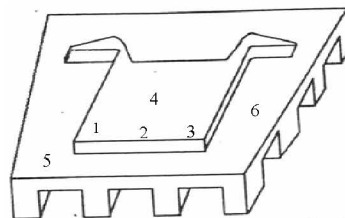


Fig. 5. Microstructure of bull's eye graphite in the fine pearlitic matrix, (Nital 2%).



Number	1	2	3	4	5	6
Hardness (HBN)	232.5	235.8	244.5	240	174	174

Fig. 6. Results of hardness test from different points of master mould.

*Required properties*

On the basis of the preceding arguments, requirements needed for cast iron to have good resistance to thermal shock and thermal fatigue can be established. In order to resist the thermal stresses, an iron should have low modules of elasticity, high tensile and high fatigue strength, specifically with respect to strain cycling, to withstand thermal and external stresses imposed by the design. Furthermore, if the operating temperature exceeds 500-550 °C, the iron must also have resistance to oxidation and structural changes. Finally, the iron must be economically attractive. These requirements cannot be met by any iron because some of the requirements are self-contradictory<sup>7, 8)</sup>. For example grey cast iron has very good thermal conductivity but low tensile strength. The opposite is the case with spheroidal cast iron. Observations of cracking behavior in flake graphite irons suggest that the rate-controlling step in the thermal fatigue process is the nucleation of cracks in the graphite flakes, and that the composition of the matrix structure had little influence on the resistance to cracking. However, increasing the amount of graphite and graphite flake size in grey cast iron improved crack resistance by increasing thermal conductivity and decreasing the coefficient of thermal expansion, which lowered total thermal strain on the heated surfaces. The quantity of graphite and graphite flake size in the alloyed irons was observed to be lower than that in irons which had superior resistance to thermal cracking<sup>9)</sup>. Therefore, a change of matrix structure from pearlite to martensite does not affect the temperature-dependence of the cracking for the grey cast iron moulds. In ductile cast iron the graphite morphology is spheroidal. Furthermore, any crack initiated in nodular graphite is only limited to that nodule, whereas cracks can propagate to any part of graphite in the case of grey cast iron. Therefore, in ductile cast iron crack has no way to propagate except through the matrix. Thus suitable alloying and heat treatment can improve the matrix structure and prevent the propagation of crack; and as we need a cast iron which in the heating and cooling cycles neither warps nor cracks, Bainitic ductile cast iron can be a good solution. This iron has the highest resistance to thermal shock and strength at the elevated temperatures compared with the above

said cast irons without warping in the heating and cooling cycles.

To examine the performance of suggested cast iron, we conducted short time high temperature tensile and thermal shock tests similar to working conditions of the cast iron. Also, we conducted identical experiments on pearlitic ductile cast iron to compare it with bainitic ductile cast iron.

*Results of tensile test*

Results of tensile tests of both pearlitic and bainitic ductile cast irons are given in Table 4. Tensile strength and percent elongation versus test temperatures are also shown in Figure 7 and 8. As it can be seen in these figures at all temperatures, bainitic ductile cast iron has higher tensile strength and elongation than pearlitic (one). With respect to Table 4, it is interesting to note that the difference between ultimate tensile strength and yield strength in the bainitic ductile cast iron is higher compared to pearlitic one. For instance; at 800 °C, this difference is about 25% for bainitic samples, whereas for pearlitic samples it is only about 3.47%. Also, in pearlitic alloy, this difference decreases with increasing temperature. Since fracture strength is equal to tensile strength in cast irons, as yielding starts fracture will occur in the alloy. While in bainitic alloy this difference does not change with temperature and as yielding starts, the metal is able to deform plastically and fracture will occur at stresses higher than yield strength. Also, Figure 7 indicates that with increasing temperature from 25 to 400 °C, tensile strength and elongation will increase 7% and 32.2%, respectively in the bainitic alloy, whereas these amounts are 2.5% and 30% in pearlitic alloy. At elevated temperatures both the tensile strength and elongation have decreased in both alloys. The increase in the tensile strength at 400 °C is associated with the blue brittleness that is related to dynamic strain aging occurring mainly in this range of temperatures<sup>10)</sup>. However, we also observed an increase in the percentage of elongation. Dynamic strain aging, which leads to homogeneous deformation characterized by serrated flow, is mainly relevant to the diffusion of interstitial atoms such as carbon or nitrogen towards moving dislocations.

*Table 4. Results of tensile tests of bainitic and pearlitic ductile cast irons in different temperatures.*

Temp. ( °C )	Normalized			Austempered		
	$\sigma_{ys}$ (MPa)	$\sigma_{uts}$ (MPa)	EI %	$\sigma_{ys}$ (MPa)	$\sigma_{uts}$ (MPa)	EI %
25	637.4	747.4	2.10	984.3	1272	3.00
400	569.9	766.4	3.00	896.2	1367	4.43
600	520.4	534.7	1.22	719.5	971.4	2.35
800	384.8	398.7	1.17	390.7	521.3	1.75

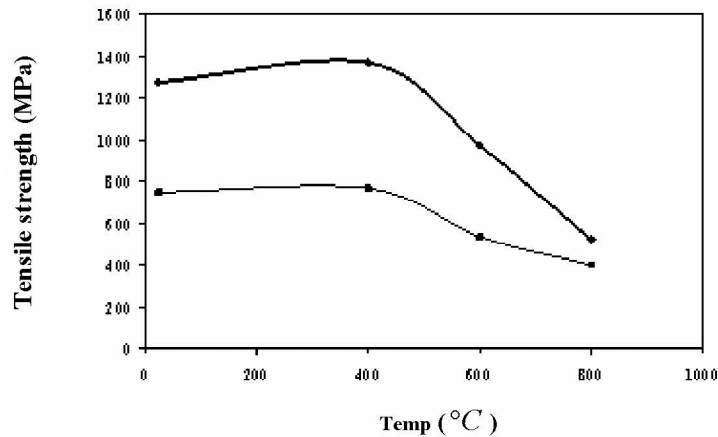


Fig. 7. Comparison of tensile strength of bainitic and pearlitic ductile cast irons in different temperatures (B: Bainite, P: Pearlite).

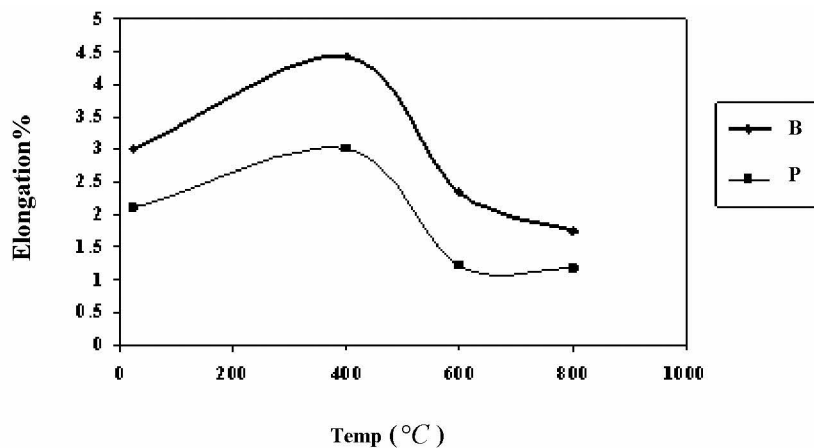


Fig. 8. Comparison of elongation of bainitic and pearlitic ductile cast irons in different temperatures (B: Bainite, P: Pearlite).

When the temperature and the strain rate are such that, the speed of interstitial atoms is more than that of dislocations, dislocations are pinned by interstitial atoms. Serrations occur due to rapid dislocation multiplication during deformation. In the process of dislocation multiplication stress increases, but once the dislocations are released the stress drops to sustain their movement until interstitial atoms diffuse and pin these mobile dislocations again<sup>10</sup>.

Regarding the fact that only the anodic part of surface of master mould during thermal cycling is heated to elevated temperatures, and almost the temperature of other parts are not higher than 500°C, one can expect that mould retains its strength in these conditions. Changes in microstructure which occur in anodic part lead to strain in this part, but bainitic microstructure in other parts of the mould that have experienced no changes prevent strain in anodic part of the master mould.

#### Results of thermal shocks

Thermal shock results are presented in Table 5. According to the results, bainitic ductile cast iron has more resistance to thermal shock compared to

pearlitic one. Microstructure of ausferrite yields high resistance to thermal shock in bainitic ductile cast iron. The cracks in samples which are cooled in air after 200 cycles and the cracks in samples which are quenched in water after 35 cycles are shown in Figure 9. From this figure, it can be seen that bainitic ductile cast iron has a good resistance to crack propagation, and after the first 1mm crack occurs, the rate of crack propagation due to heating and cooling cycles is very slow, in contrast after the first 1mm crack occurs in pearlitic ductile cast iron, the crack length reaches 5mm in next cycles and more cracks in the bridge between the holes can be seen. Figure 10 shows microscopic images of bainitic samples which are cooled in air and water after 200 heating and cooling cycles, respectively. In the structure of pearlitic samples which are cooled in the air, spherical cementite can be seen (Figure 11). During the heating, cementite in pearlitic layers breaks and tends to get a spherical shape and decomposes to carbon and iron. Decomposed carbon diffuses into cast iron and precipitates on spherical graphite. Diffusion and precipitation of carbon causes graphitization.

Table 5. Number of cycles that cause crack of 1mm length in the bridge between two holes.

Cooling of samples	Number of cycles	
	Bainitic ductile cast iron	Paerlitic ductile cast iron
air	150	100
water	27	12

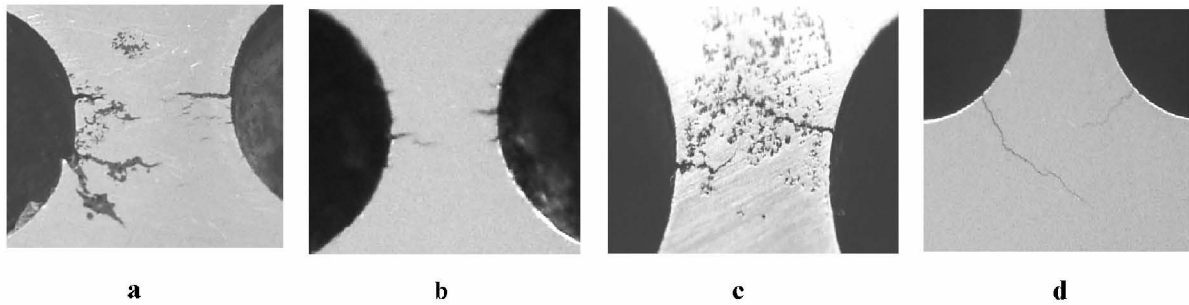


Fig. 9. (a,b) Pearlitic and bainitic samples cooled in the air after 200 cycles. (c,d) Pearlitic and bainitic samples quenched in water after 35 cycles.

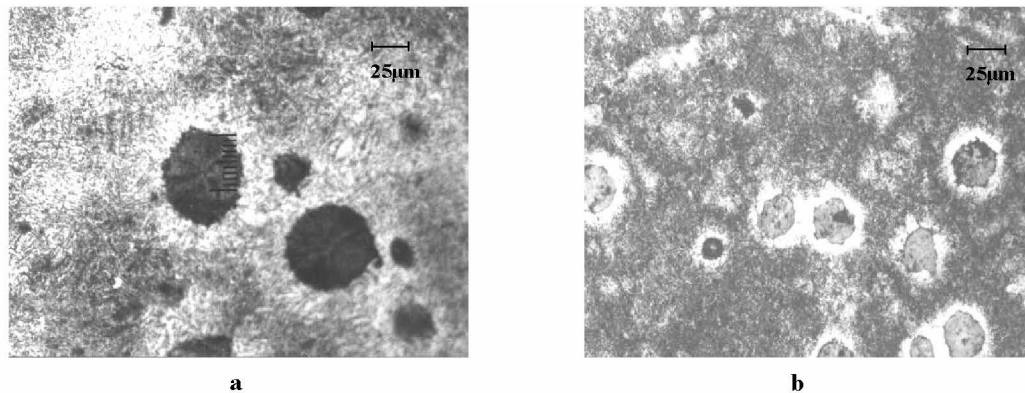


Fig. 10. Microscopic images of bainitic samples a) cooled in air b) quenched in water after 200 cycles. White areas are in the (a) ferrite and in the (b) martensite.



Fig 11. Microscopic image of pearlitic samples cooled in air after 200 cycles. Near spherical cementite can be seen in the image.

In the bainitic ductile cast iron during the heating and cooling cycles, undesirable changes of surface or bulk microstructures can occur. These can lead to the formation of elastic strains, which cause a) heavy microstructural subsurface damage because of the

graphite matrix interfaces and debonding, matrix microcracking and void growth ; b) significant amount of austenite-martensite transformation ; and c) decomposition of the reacted stable austenite, due to the localized increase in temperatures<sup>11,12</sup> . The

reacted austenite matrix in ausferrite is thermodynamically stable down to liquid nitrogen temperatures. During heating process, acicular ferrites in bainitic ductile cast iron breaks and reacted austenite phase decomposes to carbide and ferrite. Decreased carbon solubility caused by the precipitation of carbides in the reacted austenite, increased the martensite start temperature,  $M_s$ , and some of the low-carbon metastable austenite transforms to secondary martensite upon cooling (Figure 10b). This is clearly seen around the graphite nodules where carbon enrichment is the lowest. Breaking of acicular ferrites and precipitation of carbides cause hardness and strength to increase a little, but the elongation extremely decreases. By more heating cycles, acicular ferrites is converted to granular forms and precipitated carbides get more size (Figure 10a). Also a SEM image of this decomposition in the bainitic samples cooled in air after 200 cycles is shown in Figure 12. Hence hardness and strength of austempered ductile iron decrease and elongation increases. Decrease in the kinetic rate of decomposition of reacted austenite during heating can be influenced by several parameters. One of these important parameters is the amount of carbon in the reacted austenite. Decrease of carbon content in this phase delays the decomposition kinetics of the phase indicated<sup>11, 12</sup>. Since austenitizing in low temperature decreases solvent carbon content in original austenite and reacted austenite, decrease in austenitizing temperature delays decomposition kinetic<sup>11, 12</sup>.

#### Thermal modeling

The master mould was modeled by Finite Element Method (using the Ansys software) to examine the thermal conditions. The model can be used to study the effects of thermal gradients and stress concentrations. The boundary conditions for the model and the material properties of the mould

were specified in transient state at constant temperature of  $1083^{\circ}\text{C}$ . The thermal contour after 20 minutes is shown in Figure 13. This figure shows that microstructural changes can occur only in the anodic part of the mould. This is due to the fact that this part of the mould has experienced higher temperatures (above  $700^{\circ}\text{C}$ ) compared to the other parts of the mould (which have experienced temperatures lower than  $500^{\circ}\text{C}$ ). Therefore, only the strength and ductility of anodic part of the mould have changed. Also, stress contour which developed due to thermal gradient has been shown in Figure 14.

The maximum stress is in the regions where fracture occurs (Figure 15). The temperature and stress contours showed a good agreement with experimental results.

#### Recommendations

According to the results obtained, the bainitic ductile cast iron, as compared to pearlitic ductile cast iron, has more resistance to thermal shock. So, this alloy is a better choice for the master mould. Based on experiments conducted, we proposed the following composition (in wt %):

**C 3-3.3% , Si 1.8-2.2% , Mn 0.5-0.8% , Ni 3-4.5% , Mo 0.6-0.8% , Cr 0.2%**

This alloy has a bainitic structure in the as cast condition because of high Ni and Mo content. Also, the expected mechanical properties are:

Tensile strength: 1350-1400 MPa

Hardness: 350-420 HV

Elongation%: 1- 2%

If this alloy is heated to a temperature higher than austenitizing temperature and cooling from this temperature, bainitic microstructure will be obtained again and no microstructural changes such as those changes took place in ADI will occur in this alloy. We can expect life of 150-200 cycles from bainitic master mould.

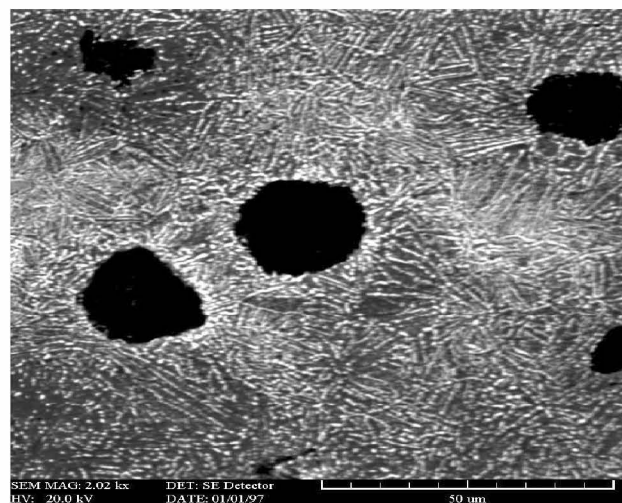


Fig. 12. SEM micrograph of ausferrite phase. Acicular ferrites are broken and transformed to granular ferrites which are present around graphite nodules.



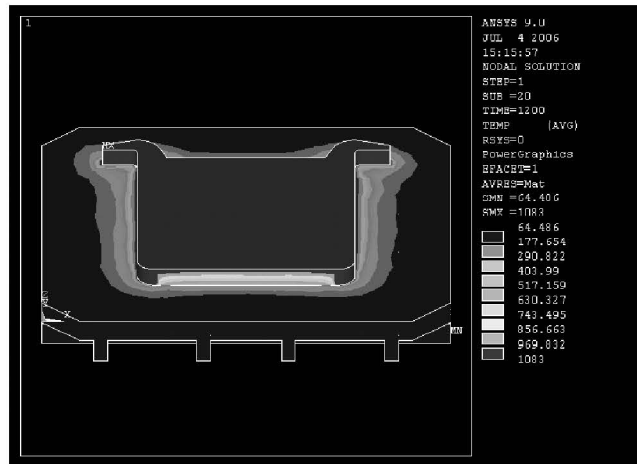


Fig. 13. Thermal contour of master mould after 20 minutes (temperature of surface is 1083°C ).

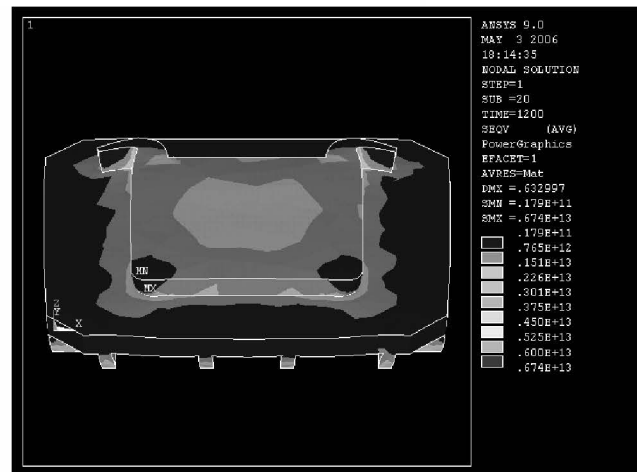


Fig. 14. Stress contour in master mould after 20 minutes, maximum and minimum stress are indicated.

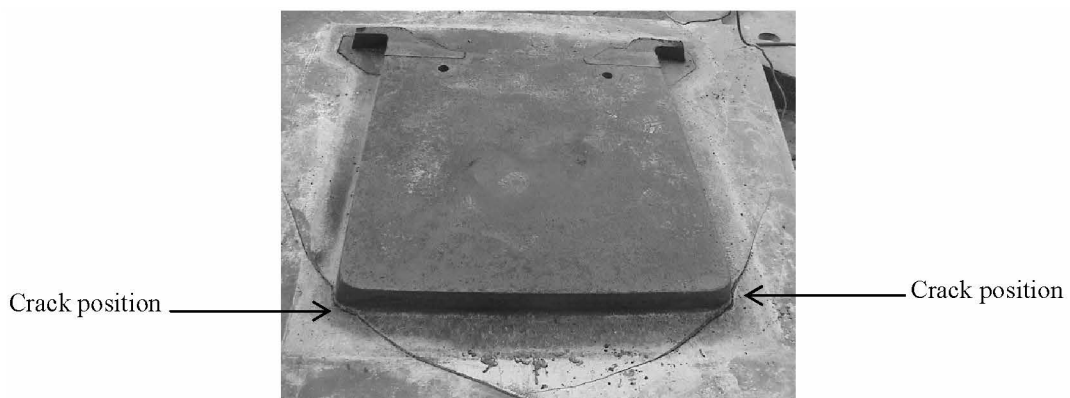


Fig. 15 Crack initiates and develops in the master mould.

### Conclusions

1- According to the experimental data, thermal shock and fatigue are the main reasons for the master mould failure.

2- Microstructure of anodic part which is in contact with molten copper is bull's eye graphite in the fine pearlitic matrix.  
 3- Hardness of anodic part is higher than that of the other parts of the mould because of periodic contact

with molten copper which induces microstructural changes.

4- The bainitic ductile cast iron has higher strength and ductility than pearlitic one at elevated and room temperatures.

5- Based on the results of tensile test, the difference between tensile strength and yield strength in bainitic cast iron is higher than pearlitic cast iron, so we observed plastic strain after yielding in the bainitic cast iron, while in pearlitic cast iron fracture occurs after yielding.

6- Bainitic alloy has more resistance to thermal shock than pearlitic alloy.

7- The results of Finite Element modeling have a good agreement with experimental results.

#### **Acknowledgement**

The authors wish to appreciate Sarcheshmeh copper complex plants for the financial aids towards this work.

#### **References**

- [1] J. M. Gallardo et al, Eng. Failure Analy. 13 (2006), 292.
- [2] C. P. Cheng, T. S. Lui, L. H. Chen, Mater. Sci. Tech., 20 (2004), 243.
- [3] "Standard Methods and Definitions for Mechanical Testing of Steel Products" A370, Annual ASTM, Philadelphia (1984), 56.
- [4] R. B Gundluch: AFS Trans, 91 (1983), 389.
- [5] I. A Kamenichny, Short Handbook of Heat Treatment. Mir published (1969), 156.
- [6] S. Y. Buni, N. Raman, Seshan, Sadhana, 29 (2004), 117.
- [7] K. Roehrig, AFS Trans , 86 (1979), 75.
- [8] K. Nyamekye, S. Wei, K. M. Martinez, AFS Trans. 105 (1997), 557.
- [9] M. M. Shea, AFS Trans , 86 (1978), 23.
- [10] O. Celik et, al ISIJ Int. 43 (2003), 1274.
- [11] G. Nadkarni, S. Gokhale, J. D. Boyd, AFS Trans., 104 (1996), 985.
- [12] J. M. Massone, R. E. Boeri, J. A. Sikora, Int. J. Cast Metals. Res., 9 (1996), 79.